Microstructures and Mechanical Properties of Friction Stir Spot Welded Aluminum Alloy AA2014

S. Babu, V.S. Sankar, G.D. Janaki Ram, P.V. Venkitakrishnan, G. Madhusudhan Reddy, and K. Prasad Rao

Friction stir spot welding (FSSW) is a relatively recent development, which can provide a superior alternative to resistance spot welding and riveting for fabrication of aluminum sheet metal structures. In the current work, FSSW experiments were conducted in 3-mm thick sheets of aluminum alloy 2014 in T4 and T6 conditions, with and without Alclad layers. The effects of tool geometry and welding process parameters on joint formation were investigated. A good correlation between process parameters, bond width, hook height, joint strength, and fracture mode was observed. The presence of Alclad layers and the base metal temper condition were found to have no major effect on joint formation and joint strength. Friction stir spot welds produced under optimum conditions were found to be superior to riveted joints in lap-shear and cross-tension tests. The prospects of FSSW in aluminum sheet metal fabrication are discussed.

1. Introduction

Producing reliable joints in aluminum alloys on a consistent basis using resistance spot welding is a challenging task. Consequently, aluminum sheet metal structures are often fabricated by riveting. Friction stir spot welding (FSSW), an emerging solid-state spot welding process, is a potential alternative to riveting.

FSSW was developed by Mazda Motor Corporation and Kawasaki Heavy Industries, which was an off-shoot of friction stir welding (FSW) (Ref 1). In this process (Fig. 1), welds are produced using a non-consumable tool, consisting of a pin and a shoulder. The tool is rotated at a constant speed throughout the process. The sheet materials that are to be joined are placed one over another in lap configuration and are tightly clamped to an anvil. The rotating tool is gradually plunged into the sheets until the shoulder comes in contact with the upper sheet surface. Typically, the pin length is so chosen that it sufficiently penetrates into the lower sheet. Heat generated by friction softens the material being welded. The softened material is stirred resulting in intimate mixing of the upper and lower sheet materials. After a certain dwell time, the tool is withdrawn (no tool translation is involved). The result is a spot weld produced in the solid state between the upper and lower sheets with a central hole (pin hole or exit hole). Some interesting variations

of FSSW have been developed in the past few years, as researchers attempt to refine the process with an aim to eliminate the exit hole or to improve the bond area and joint strength (Ref 2-5). These process modifications, however, necessitate sophisticated equipment and tools. Some of the advantages of FSSW relative to resistance spot welding and riveting are (Ref 5): (i) no weld cracking or porosity problems, (ii) superior weld mechanical properties, (iii) short welding times and amenability for automation, (iv) suitability for welding dissimilar materials and sheet thicknesses, (v) reduction in overall structural weight, and (vi) large energy savings.

Much of the research to date on FSSW has been supported by the automotive industry as FSSW is considered a crucial technology for realizing aluminum alloys in auto body applications (Ref 5). There is considerable interest in the aerospace industry as well, as the use of FSSW in place of riveting in aluminum sheet metal structures can potentially result in considerable weight savings as well as reduced assembly times and costs. To date, FSSW has been studied in several different Al alloys—AA2017-T351 (Ref 6), AA2024-T351 (Ref 7), AA5754-O (Ref 8), AA5052-H34 (Ref 9) AA6060-T5 (Ref 10), AA6061-T4 (Ref 11), AA6111-T4 (Ref 12), and AA7075-T6 (Ref 13), generally in sheet thicknesses between 1 and 2 mm. FSSW has also been shown to be effective for spot welding dissimilar aluminum alloys (Ref 14, 15). Further, attempts have been made to model the FSSW process capturing the underlying thermo-mechanical phenomena (Ref 16-19). Apart from aluminum alloys, FSSW has been investigated in magnesium alloys (Ref 20, 21) and steels (Ref 22). Studies have also been carried out on FSSW of aluminum to steel (Ref 23) and aluminum to magnesium (Ref 24).

As can be expected, producing satisfactory friction stir spot welds requires that the process is carefully optimized for a given material and for a given sheet thickness combination. Earlier studies show that the choice of process parameters (tool rotational speed, tool plunge, and stir time) and tool geometry (pin profile, pin dimensions, and shoulder diameter) is crucial in FSSW (Ref 5, 7-9, 14, 25, 26). In friction stir butt welding, the central issue in process optimization is defect elimination.

S. Babu, V.S. Sankar, G.D. Janaki Ram, and K. Prasad Rao, Department of Metallurgical and Materials Engineering, Indian Institute of Technology Madras, Chennai 600 036, India; P.V. Venkitakrishnan, Liquid Propulsion Systems Centre, ISRO, Tiruvananthapuram, India; and G. Madhusudhan Reddy, Defence Metallurgical Research Laboratory, Hyderabad, India. Contact e-mail: jram@iitm.ac.in.

In FSSW, on the other hand, process optimization is generally carried out based on two microstructural parameters termed "bond width" and "hook height." These parameters, along with other relevant FSSW terminology, are defined in Fig. 2.

In FSSW, bond formation is more or less the same all around the exit hole. Therefore, on the cross section of a typical friction stir spot weld, microstructure on one side of the exit hole appears almost like a mirror image of that on the other side. Next to the exit hole on either side, there exists a region of a certain width, over which the upper and lower sheets are fully bonded. It is the width of this region that is termed the bond width. Usually, the fully-bonded region ends just outside the boundary between stir zone (SZ) and thermo-mechanically affected zone (TMAZ). Next to the fully-bonded region, a partially bonded region appears, over which the upper and lower sheets are separated by a very thin, discontinuous, wavy or irregular interface line. The partially-bonded region is usually contained within the shoulder radius. At the beginning of the partially-bonded region, because of the plunging and stirring action of the tool, the interface line separating the upper and lower sheets bends upward a little bit, forming a "hook" (Ref 5).

Earlier studies suggest that for maximizing the load-bearing capability of friction stir spot welds, it is necessary to maximize the bond width and minimize the hook height (Ref 5). However, it is not clearly known whether bond width or hook height is more critical. Similarly, aluminum alloys are often used in Alclad condition. There are no reports in open literature on FSSW of Alclad aluminum sheets. It is not known whether Alclad layers present any special problems in FSSW. Further, heat-treatable aluminum alloys are industrially used in various

temper conditions. The effects of base material temper condition are well-understood in fusion and friction stir butt welding processes (Ref 27, 28). Overaging of strengthening precipitates in the heat-affected zone (HAZ) is a serious concern in welding of heat-treatable aluminum alloys. Welding in T4 condition (solution treated + naturally aged) is often preferred to welding in T6 condition (solution treated + artificially aged to peak hardness) to minimize the problem of HAZ overaging. While FSSW can certainly result in HAZ overaging, how relevant is the problem of HAZ overaging in friction stir spot welds is not clearly known. Finally, the mechanical properties of friction stir spot welds are seldom compared one-to-one with those of riveted joints. Such a comparison would be very useful in assessing the prospects of FSSW.

In the current work, FSSW experiments were conducted in a heat-treatable aluminum alloy in T4 and T6 conditions, with and without Alclad layers. Welds were produced using several different tools over a broad range of process parameters to evaluate their influence on bond width and hook formation. The effects of Alclad layers and base material temper condition were investigated. Lap-shear and cross-tension tests were conducted on joints produced by FSSW and riveting. Failure modes in friction stir spot welds were analyzed.

2. Experimental Details

3-mm thick Alclad sheets of Al-Cu-Mg alloy AA2014 in T4 and T6 conditions were used in the current study. Alloy AA2014 is extensively used in aerospace sheet metal structures, such as inter-stage skin panels. The chemical composition of the base material is listed in Table 1, along with the specified composition for alloy 2014 as per ASTM B209M. The base material sheets consisted of a 100-µm thick clad layer of pure aluminum on either side. FSSW experiments were conducted using a commercially available friction stir welding machine (Eta Technologies of Bangalore, India) at Defence Metallurgical Research Laboratory, Hyderabad, India.

In the first round of FSSW experiments, seven different tools were used (Table 2). All the tools had a straight cylindrical pin with a flat shoulder (Fig. 3). All the experiments in this round were conducted in alloy 2014-T4 Alclad sheets. Welds were produced over a broad range of process parameters (Tool
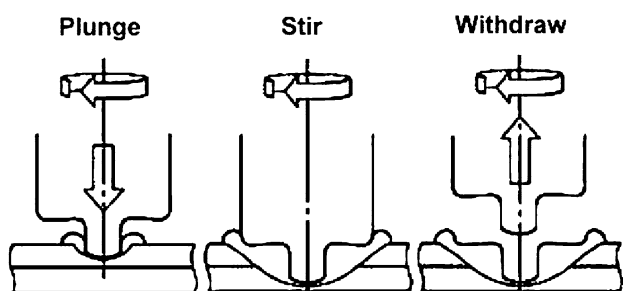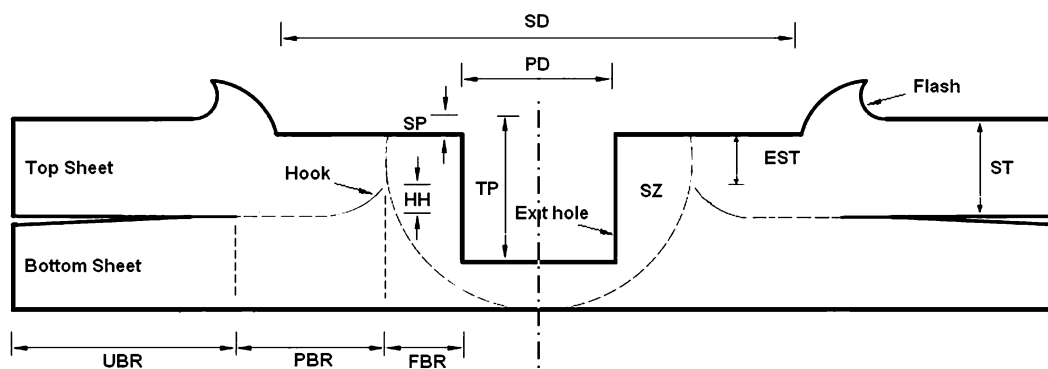

Fig. 1 Schematic illustration of FSSW

HH - Hook Height; FBR - Fully Bonded Region; PBR - Partially Bonded Region; UBR - Unbonded region; SZ - Stir Zone; EST - Effect Sheet Thickness; ST - Sheet Thickness, SP - Shoulder Plunge; TP - Tool Plunge; SD - Shoulder Diameter; PD - Pin Diameter

**Fig. 2** Schematic cross-sectional view of a friction stir spot weld

Table 1 Chemical composition of alloy AA2014 (in wt.%)

Element	Specified (ASTM B209M)	Obtained
Cu	3.9-5.0	4.75
Si	0.5-1.2	0.76
Mn	0.4-1.2	0.84
Mg	0.2-0.8	0.66
Fe	0.7 max	0.52
Zn	0.25 max	0.15
Ti	0.15 max	0.10
Cr	0.1 max	0.06
Others	0.15 max	0.08
Al	Bal	Bal

Table 2 Tools used in the first round of FSSW experiments

Tool #	Pin length, mm	Pin diameter, mm	Shoulder diameter, mm
Tool 1	5.5	5	15
Tool 2	5	5	15
Tool 3	4.5	5	15
Tool 4	5	5	12
Tool 5	5	4	12
Tool 6	4.5	4	12
Tool 7	4.5	4	10

The pin is straight cylindrical in all cases
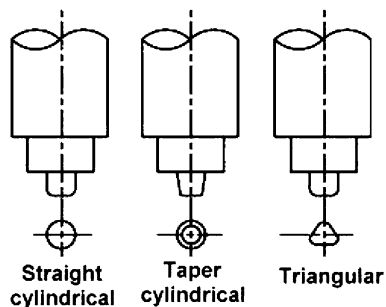
Fig. 3 Pin profiles used in the current study

rotational speed: 1000-2000 rpm, Plunge depth: 0.1-0.3 mm in excess of pin length, Stir time: 5-40 s. A constant plunge rate of 0.5 mm/s was used in all the cases. The aim was to determine the optimum tool dimensions and process parameters. Figure 4 shows the spot welds produced using Tool # 2 by various process parameter combinations. All the welds were sectioned and prepared for microstructural examination following standard metallographic practices. Samples were examined in both as-polished and etched condition (Keller's reagent). The bond width and hook height were carefully measured in all the welds using a light microscope. Based on microstructural observations, a pin diameter of 5 mm and a pin length of 5 mm and a shoulder diameter of 15 mm were considered appropriate for producing spot welds in 3-mm thick sheets of alloy 2014. Similarly, a process parameter combination of 1500-rpm tool rotational speed, 5.1-mm tool plunge, and 10-s stir time was

Fig. 4 Spot welds produced using Tool # 2 by various process parameter combinations

found to produce the best results. All subsequent FSSW experiments were carried out using the above tool dimensions and process parameters.

In the second round of FSSW experiments, welds were produced in alloy 2014-T4 Alclad sheets using a taper cylindrical tool and a triangular tool (Fig. 3; Table 3). Welds produced using these tools were comparatively assessed using those made using Tool # 2. All the welds were metallographically examined for bond width and hook height. Lap-shear tests were carried out on welds produced using these three tools (Tools # 2, 8, and 9). In addition, welds produced using Tool # 9 (triangular tool) were subjected to cross-tension tests. Both the tests were carried out as per ANSI/AWS/SAE/D8.9-97. A universal testing machine was used for this purpose. Typical lap-shear and cross-tension test specimens produced by FSSW are shown in Fig. 5a and c, respectively. An overlap length of 40 mm was used in all the cases. Lap-shear and cross-tension tests were also conducted on riveted joints (Fig. 5b and d), produced as per standard shop-floor practices (cold heading using a pneumatic hammer). The rivets used were 4 mm in diameter and 12 mm in length and were made of a commercial Al-Cu-Mg alloy V-65 (Fig. 5d, inset). After lap-shear and cross-tension testing, failure modes were analyzed in various joints. Based on microstructural studies and lap-shear tests, Tool # 9 (triangular tool) was found to produce the best results. All subsequent FSSW experiments were carried out using this tool.

In the third round of FSSW experiments, welds were produced in 3-mm thick Alclad sheets of alloy 2014-T6. Further, welds were produced in alloy 2014-T4 sheets after removing the Alclad layers on mating sheet surfaces by surface grinding. The surface roughness of bare sheets (R_a: 1.28 ± 0.2 μm) was not significantly different from that of Alclad sheets (R_a: 0.73 ± 0.15 μm). These welds were also subjected to microstructural studies and lap-shear tests. Welds produced under optimum conditions were examined using a scanning electron microscope (SEM) equipped by Energy Dispersive Spectroscopy (EDS). Vickers microhardness measurements

Table 3 Tools used in the second round of FSSW experiments

Tool #	Pin profile and dimensions
Tool 8	Taper cylindrical pin, 5 mm dia (at shoulder), 4 mm dia (at pin end), 5 mm pin length, 15 mm shoulder diameter, flat shoulder
Tool 9	Triangular pin (equilateral) with 5.25 mm base and 4.0 mm height, 0.25 mm edge chamfer on all corners, 5 mm pin length, 15 mm shoulder diameter, flat shoulder
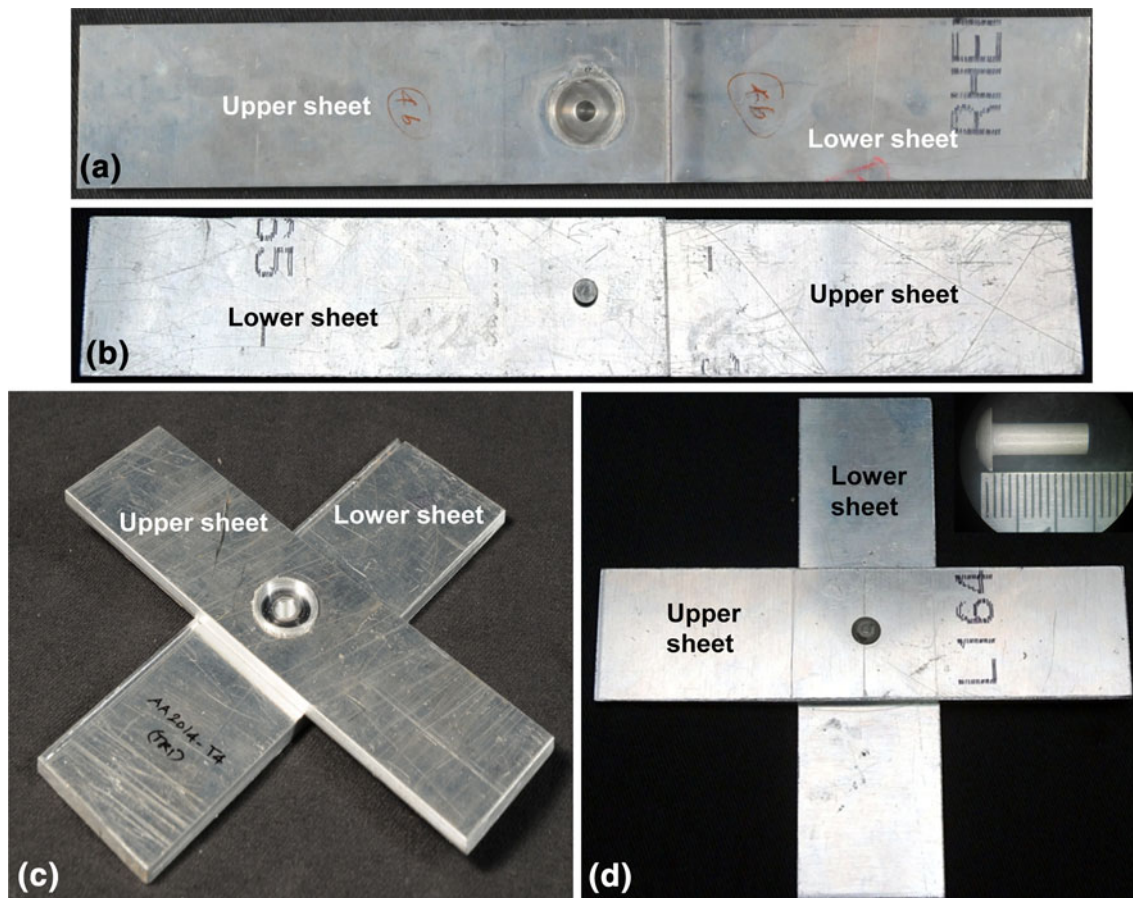
Fig. 5 Typical lap-shear and cross-tension test specimens: (a) lap-shear, FSSW, (b) lap-shear, riveting, (c) Cross-tension, FSSW, (d) cross-tension, riveting (a rivet is shown in the inset)

(30-g load applied for 15 s) were also carried out in various regions of these welds.

3. Results and Discussion

### 3.1 Effects of Tool Geometry and Process Parameters

Figure 6a shows the optical microstructure of the base material in T4 condition (longitudinal section). The average grain size of the base material was approximately 30 μm. The base material consisted of a large number of undissolved second-phase particles (4-8 μm in size) (Fig. 6b). Based on EDS analysis, these particles were confirmed to be Al_2Cu (θ) and Fe-Mn-Al intermetallics. The optical and SEM microstructures of the T6 base material were very similar to those of the T4 base material. However, it is known that alloy 2014 in T6 condition contains well-developed strengthening precipitates of

λ' ($Al_5Cu_2Mg_8Si_5$) and θ' (Al_2Cu) phases, while the material in T4 condition contains only GP zones (Ref 29). Consequently, the base material in T6 condition possesses higher strength than in T4 condition. In the current study, an average hardness of HV 104 and HV 116 was measured on the base material in T4 and T6 conditions, respectively.

In the first round of FSSW experiments, the effects of tool dimensions and process parameters were systematically studied. All the experiments were conducted in 3-mm thick Alclad sheets of alloy 2014-T4. Welds produced using various tools and process parameter combinations were sectioned and metallographically examined for bond width and hook height. The macro- and microstructures of the best weld obtained in the first round of experiments are shown in Fig. 7. As in the case of friction stir butt welds, friction stir spot welds show three distinct microstructural regions: SZ, TMAZ, and HAZ. In the SZ, very fine, recrystallized grains were observed in all the welds. The TMAZ showed severely deformed, unrecrystallized
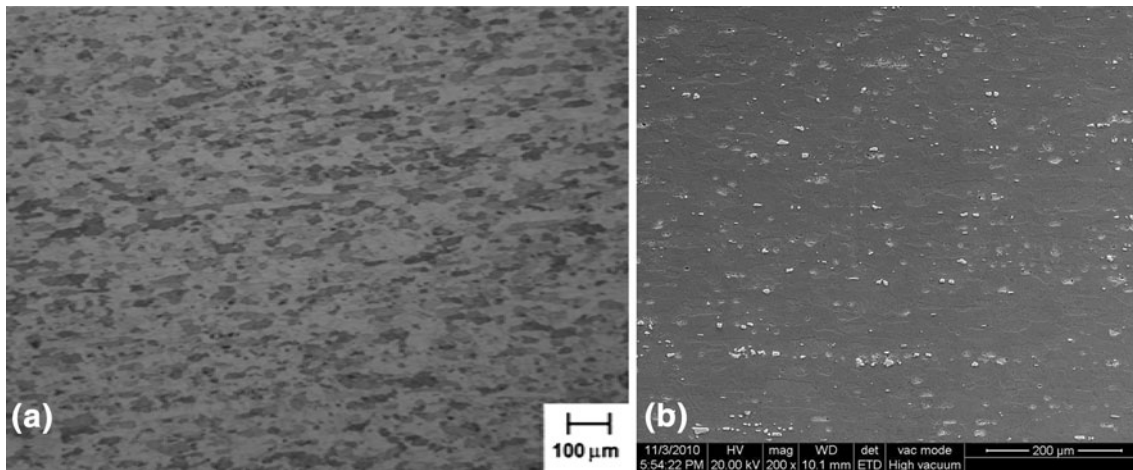
Fig. 6 Microstructures of AA2014-T4 base material: (a) Optical micrograph and (b) SEM secondary electron image
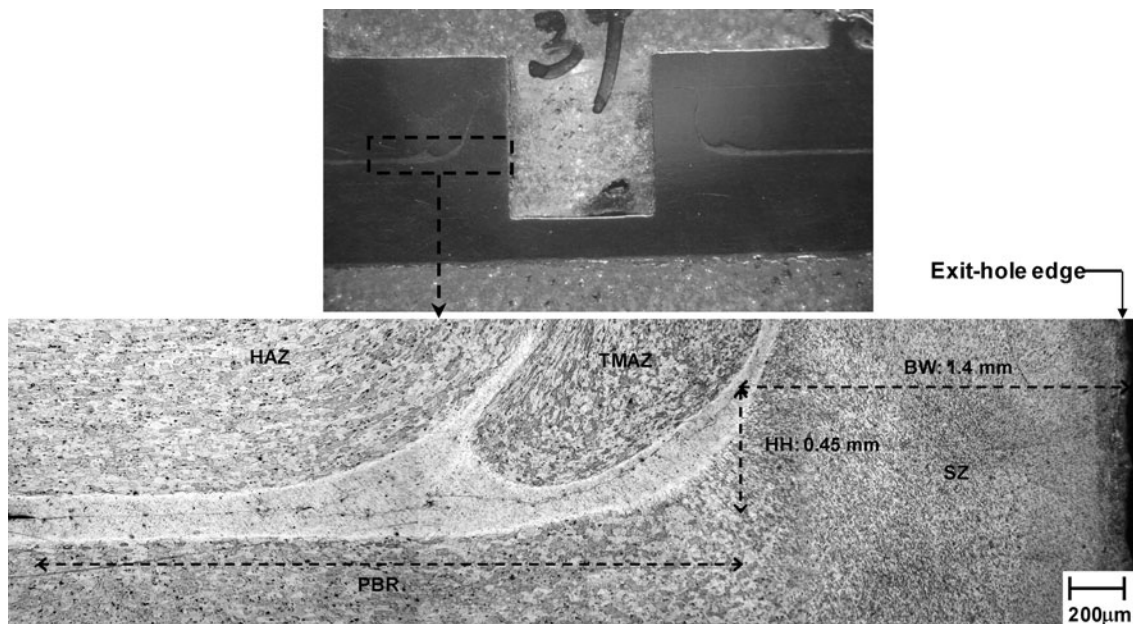
Fig. 7 Macro- and microstructures of a friction stir spot weld made using Tool # 2 using 1500-rpm tool rotational speed, 5.1-mm tool plunge, and 10-s stir time

grains. The HAZ showed no significant grain coarsening. With regard to bonding, all the welds showed distinct fully bonded and partially bonded regions. All the welds showed streaks of Alclad extending into the SZ pointing toward the weld top side, as can be seen in Fig. 7. The hook is contained within the Alclad streaks. The bond width and hook height were found to vary significantly among the welds. Broadly, the following trends were noticed:

a. The bond width increased with increase in pin length from 4.5 mm to 5 mm (Fig. 8). With increase in pin length, more material is plastically deformed leading to bonding over a wider region. However, further increase in pin length to 5.5 mm did not significantly benefit the

bond width, but led to significant increase in the hook height. For 3-mm thick sheets of alloy 2014, a pin length of 5 mm was found to be appropriate. Similarly, tools with 5-mm pin diameter were found to produce better results compared to those with 4-mm pin diameter.

b. The bond width increased with increase in shoulder diameter from 12 to 15 mm (compare Fig. 9 with Fig. 8a). Increase in shoulder diameter was also found to result in a wider partially bonded region. The amount of heat generated during FSSW can be expected to increase with increasing shoulder diameter, which helps plastic deformation and bonding over a wider region. For a pin diameter of 5 mm, a shoulder diameter of 15 mm was found to be appropriate. A shoulder-to-pin diameter ratio
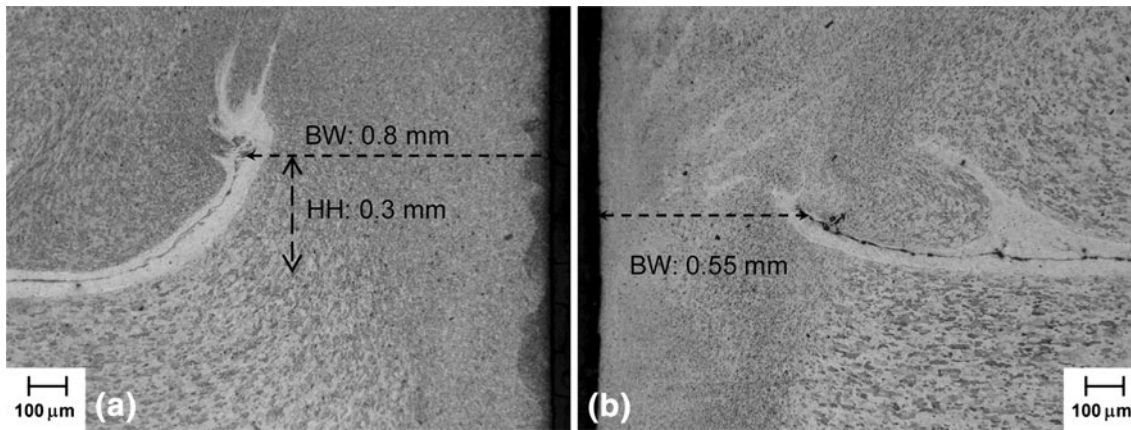
Fig. 8 Welds microstructures showing the effect of pin length on bond width: (a) Tool # 2, 5.1 mm tool plunge; (b) Tool # 3, 4.6 mm tool plunge. Both the welds were made using 1100-rpm tool rotational speed and 10-s stir time
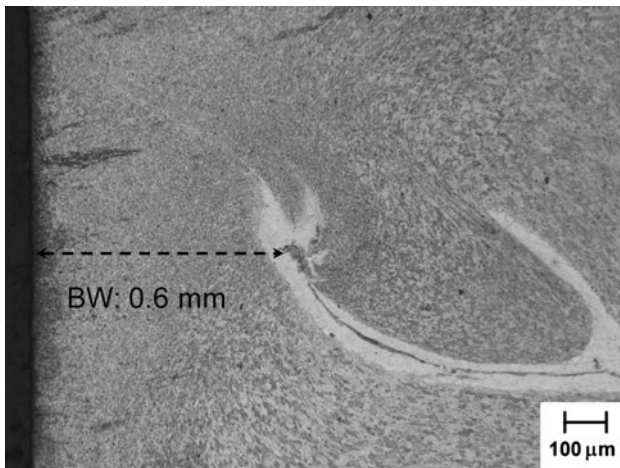
Fig. 9 Microstructure of a friction stir spot weld made using Tool # 4 (1100 rpm tool rotational speed, 5.1-mm tool plunge and 10-s stir time)

of 2.5-3 is commonly used in friction stir welding (Ref 30).

c. With regard to tool plunge, the optimum setting appears to be 0.1 mm in excess of pin length—just sufficient to insure good frictional contact between the tool shoulder and the upper sheet. Increase in plunge depth beyond this will lead to increased hook height, which is undesirable (Fig. 10).

d. The bond width increased with the tool rotational speed up to 1500 rpm (compare Fig. 11 with Fig. 9). Further increase in the tool rotational speed did not improve the bond width. Use of very high tool rotational speeds can result in excessive heating, which is undesirable.

e. The bond width increased with increase in stir time from 5 to 10 s (compare Fig. 12 with Fig. 8a). However, increase in stir time beyond 10 s did not improve the bond width significantly. From the points of view of heat input and productivity, it is desirable to keep stir time as low as possible. Very brief stir times, however, can lead to insufficient mixing of the upper and lower sheet materials.

Based on the above, a pin diameter of 5 mm and a pin length of 5 mm and a shoulder diameter of 15 mm were considered appropriate for producing spot welds in 3-mm thick sheets of alloy 2014. Similarly, a process parameter combination of 1500-rpm tool rotational speed, 5.1-mm tool plunge, and 10-s stir time was found to produce the best results.

In the second round of FSSW experiments, welds were produced in alloy 2014-T4 Alclad sheets using straight cylindrical (Tool # 2), taper cylindrical (Tool # 8), and triangular (Tool # 9) tools. The process parameters used were the same for all the tools (1500-rpm tool rotational speed, 5.1-mm tool plunge, and 10-s stir time). All the welds were examined for hook height and bond width. Welds produced using the taper cylindrical tool showed practically no hook formation (Fig. 13); however, the bond width in these welds was considerably lower (around 1 mm) than that in the welds produced using the straight cylindrical tool (around 1.4 mm). On the other hand, no significant differences were observed with regard to hook height between the welds made using the straight cylindrical and triangular tools. However, welds produced using the triangular tool showed significantly higher bond width (up to 2.3 mm) compared to those made using the straight cylindrical tool. Figure 14 shows the macro- and microstructures of the welds produced using the triangular tool.

The effects of tool geometry have been extensively studied in friction stir butt welding (Ref 28, 30). Similarly, a few investigations are available on the effects of tool geometry on metal flow in FSSW (Ref 8, 25, 31, 32). In general, the desirable pattern of metal flow in FSSW seems to be different from that in friction stir butt welding. Yang et al. (Ref 33) discussed the nature of metal flow in FSSW. As the pin plunges into the sheets placed one over another, it extrudes the material downward, causing the adjoining lower sheet material to move upward. Subsequently, as the rotating shoulder comes in contact with the upper sheet, three distinct regions develop— (i) the flow transition zone immediately underneath the tool shoulder, (ii) the SZ around the pin, and (iii) the torsion zone underneath the pin—due to a combination of rotational, horizontal, and vertical motions of the plasticized material. Intense mixing of the upper and lower sheet materials takes place in the flow transition zone, and the intermingled materials flowing from the flow transition zone contribute to the formation of the SZ.
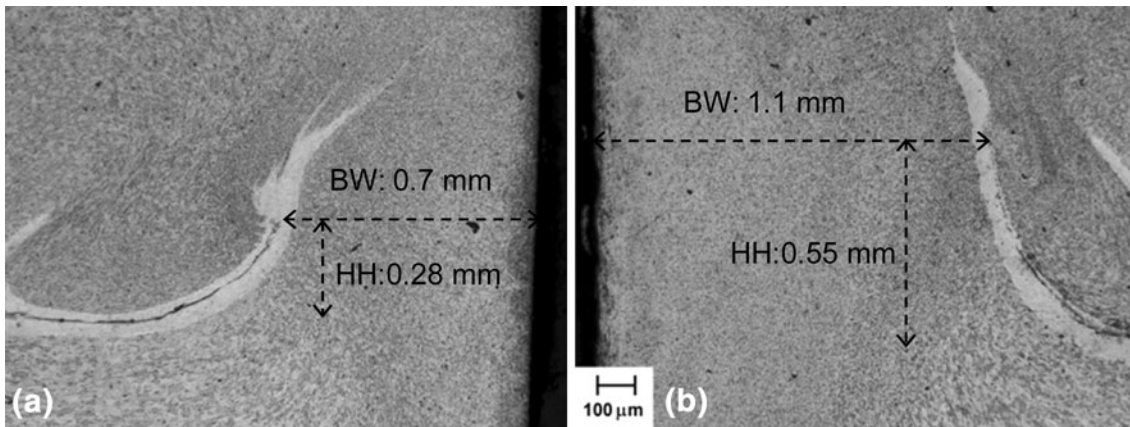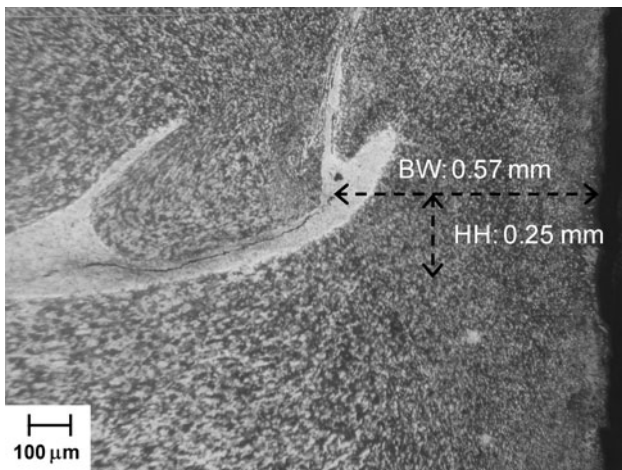
Fig. 10 Weld microstructures showing the effect of tool plunge on hook height: (a) 5.1-mm tool plunge and (b) 5.3-mm tool plunge. Both the welds were made using Tool # 5 using 1500-rpm tool rotational speed and 20-s stir time
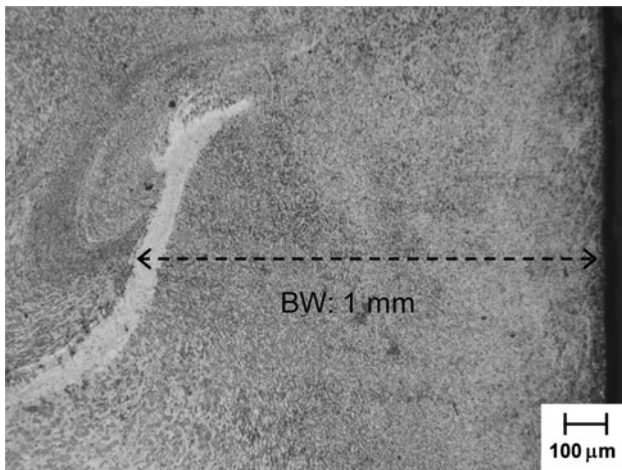
Fig. 11 Microstructure of a friction stir spot weld made using Tool # 4 using 1500-rpm tool rotational speed, 5.1-mm tool plunge, and 10-s stir time
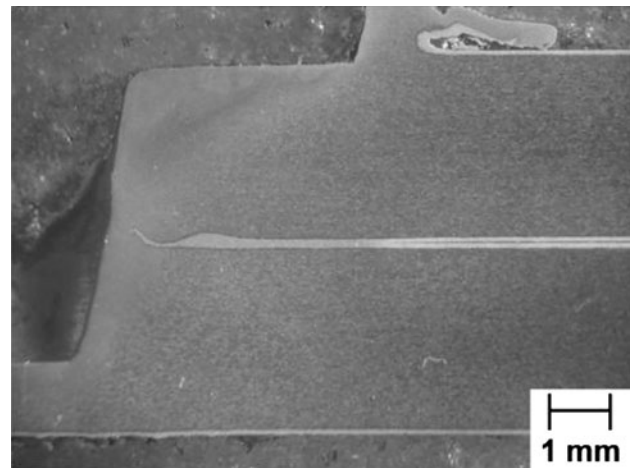
Fig. 13 Macrostructure of a friction stir spot weld produced using the taper cylindrical tool (Tool # 8)

The hook height and bond width in friction stir spot welds are influenced by the nature and extent of metal flow around the pin. Buffa et al. (Ref 34) investigated metal flow patterns in aluminum alloy friction stir butt welds made using straight cylindrical and taper cylindrical tools. According to them, welding using a straight cylindrical tool results in an upward metal flow around the pinwhile welding using a taper cylindrical tool results in a downward metal flow, especially at higher pin angles. Such a downward metal flow is particularly beneficial in the context of FSSW as it helps minimize the hook height. Similar findings were reported by Hirasawa et al. (Ref 32) in an investigation on the effect of tool geometry on plastic flow during FSSW. Welds produced in the current work using the taper cylindrical tool indeed showed substantially lower hook height, but their bond width was unsatisfactory. Incorporation of threads and increase in pin diameter might help obtain better results using the taper cylindrical tool.

The current study shows that a triangular tool is better suited for FSSW, which is in agreement with the findings of earlier investigations (Ref 8, 31, 32). Badarinarayan et al. (Ref 31) and Hirasawa et al. (Ref 32) discussed the differences in metal flow during FSSW using straight cylindrical and triangular tools.
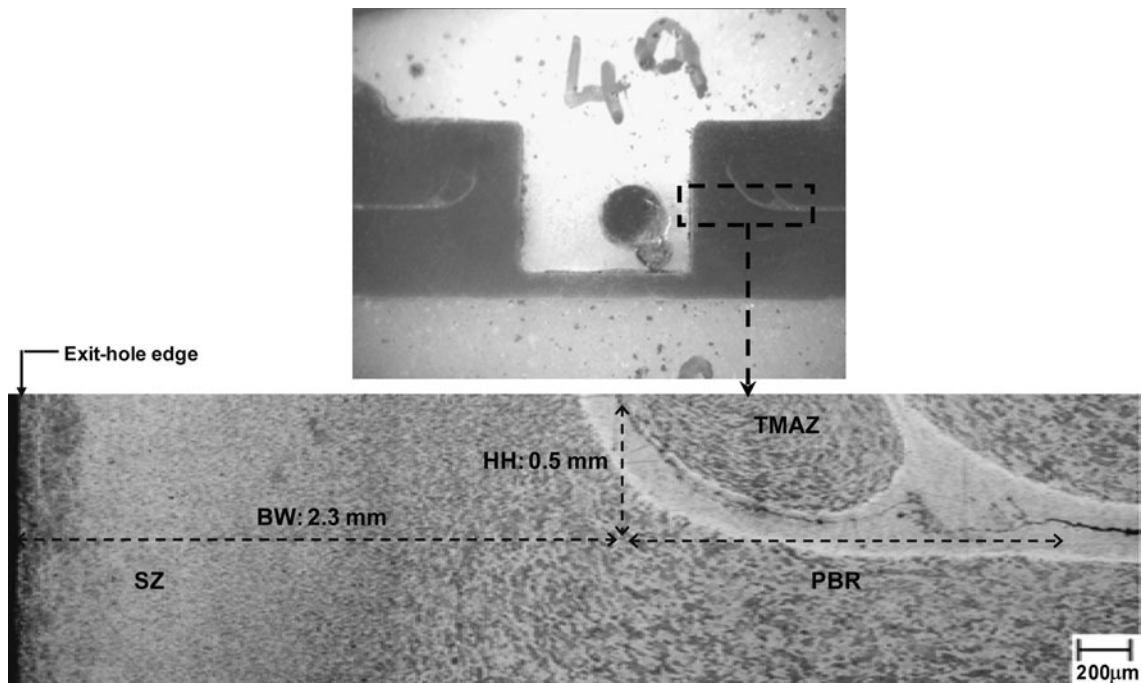

Fig. 12 Microstructure of a friction stir spot weld made using Tool # 2 using 1100-rpm tool rotational speed, 5.1-mm tool plunge, and 5-s stir time

Fig. 14 Macro- and microstructures of a friction stir spot weld made using the triangular tool (Tool # 9)
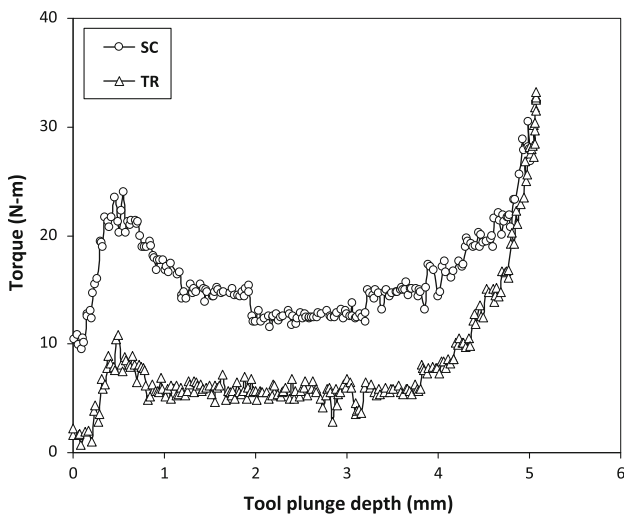

Fig. 15 Variation of torque on the tool with plunge depth (SC: straight cylindrical, TR: triangular)

In short, during FSSW using a straight cylindrical tool, the pin causes the plasticized material to flow around its own axis (rotational flow). In contrast, in addition to the rotational flow, a triangular pin causes the material in the vicinity of the pin to move back and forth in the radial direction. Consequently, plastic deformation occurs more intensely and over a wider region around the pin. Use of a triangular tool can thus help maximize the bond width in friction stir spot welds. While earlier investigators reported considerably reduced hook height using triangular tool, welds made using the straight cylindrical and triangular tools in the current study showed more or less the same hook height (around 0.5 mm). Figure 15 shows the variation of the torque on the tool (which is a measure of the shear stress acting on the tool) with plunge depth for straight cylindrical and triangular tools. As can be seen, in both cases, the torque initially increased with increasing plunge depth (up to a plunge depth of 0.5 mm) and then it decreased and remained more or less constant (up to a plunge depth of 3 mm). The torque increased continuously with further increase in plunge depth, reaching a maximum when the plunge depth approached 5 mm (i.e., when the shoulder came in contact with the upper sheet surface). More importantly, the torque on the triangular tool was significantly lower throughout the plunge stage compared to that on the straight cylindrical tool, suggesting more efficient material stirring using the triangular tool. These results are consistent with the observations reported in an earlier study by Badarinarayan et al. (Ref 8). Lower welding torque is generally considered beneficial in friction stir welding as it means reduced power consumption during welding and increased tool life (Ref 28).

Spot welded joint using Tools # 2, 8, and 9 in 3-mm thick AA2014-T4 Alclad sheets were subjected to lap-shear testing along with riveted joints. Cross-tension tests were conducted on spot welded (with triangular tool) and riveted joints. The results are given in Table 4. As can be seen, friction stir spot welded specimens withstood significantly higher loads compared to riveted joints in both lap-shear and cross-tension tests. The current study thus confirms that FSSW can provide an alternative to riveting for fabrication of aluminum sheet metal structures.

Among the three weld specimens, welds produced using the triangular tool showed the highest load-bearing capability, followed by those made using the straight cylindrical tool. As noted earlier, welds made using the triangular tool showed the highest bond width (2.3 mm), followed by those made using the straight cylindrical tool (1.4 mm). Welds made using the taper cylindrical tool showed the lowest bond width (1 mm). A clear relationship between lap-shear strength and bond width can thus be seen in friction stir spot welds. The results suggest that the lap-shear strength of friction stir spot welds is more a

Table 4 Results of lap-shear and cross-tension testing (based on six tests in each case)

Base material	Specimen	Average failure load, kN
Lap-shear tests		
AA2014-T4 with Alclad	Spot weld, Tool # 2	8.0 ± 0.4
	Spot weld, Tool # 8	6.5 ± 0.6
	Spot weld, Tool # 9	9.2 ± 0.3
	Riveted joint	3.4 ± 0.3
AA2014-T4 without Alclad	Spot weld, Tool # 9	8.9 ± 0.5
AA2014-T6 with Alclad	Spot weld, Tool # 9	9.0 ± 0.4
Cross-tension tests		
AA2014-T4 with Alclad	Spot weld, Tool # 9	6.8 ± 0.5
	Riveted joint	5.5 ± 0.4
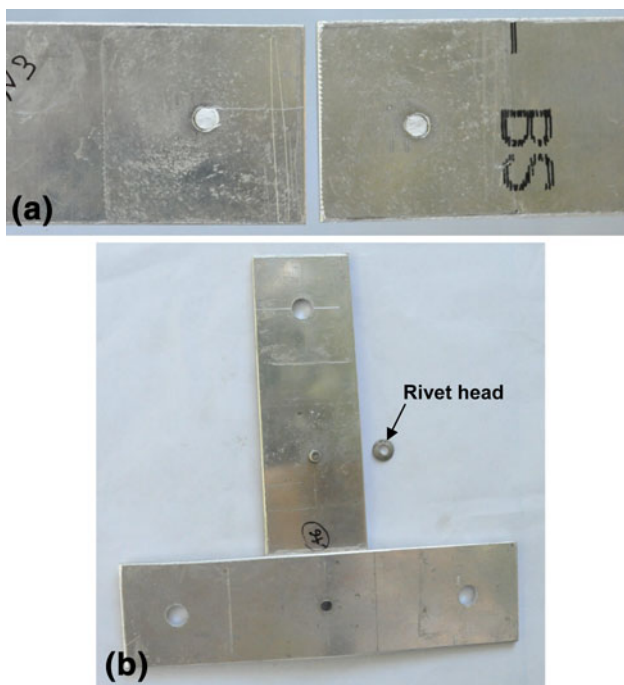
Fig. 16 Failure modes in riveted joints: (a) lap-shear and (b) cross-tension

function of the bond width than the hook height. On the contrary, in earlier investigations on FSSW (Ref 5, 8, 25, 35), lap-shear strength was found to be more sensitive to the hook height than the bond width. It must be noted, however, that most of the earlier studies were conducted using relatively thinner sheets (<2 mm). Whether bond width or hook height is more important for friction stir spot welds appears to be dependent on the base material thickness. In thicker sheets, as long as the hook is not excessively high, the weld lap-shear performance seems to be primarily determined by the bond width.

Failure modes in spot welds and riveted joints under lap-shear and cross-tension loading were investigated. In lap-shear tested riveted joints, the rivet was found to get sheared across (Fig. 16a); whereas, in cross-tension tests, the rivet head was found to come off (Fig. 16b). These modes of failure in lap-shear and cross-tension tests are normal in riveted joints. In the

case of lap-shear tested spot welds, the crack appeared to initiate from the hook in the upper sheet on the loading side of the weld in the upper sheet and run across the exit hole in a roughly 45° orientation, leading to final fracture (across the SZ) along the original sheet interface on the other side of the weld (Fig. 17). Similar observations were reported by Yin et al. (Ref 21) in friction stir spot welded Mg alloy AZ31 sheets and Lin et al. (Ref 36) in friction stir spot welded aluminum 6111-T4 sheets. SEM examination of the fracture surfaces (in the final fracture portion) revealed elongated dimples, characteristic of shear failures in ductile mode (Fig. 17e).

In cross-tension tests, spot welded specimens were observed to fail in weld pull-out mode (Fig. 18), which is the most desirable failure mode in spot welds. As can be seen, fracture occurred around the weld originating from the hook, which is consistent with the observation reported by Tozaki (Ref 25). In contrast to lap-shear, the performance of a spot weld under cross-tension loading seems to be governed more by the hook height. Further studies are however necessary to confirm this suggestion.

3.2 Effect of Alclad Layers and Base Material Temper Condition

In order to investigate the effects of Alclad layers on bond formation and joint performance, friction stir spot welds were produced (using the triangular tool) in alloy 2014-T4 sheets after removing the Alclad layers on mating sheet surfaces by surface grinding. The process parameters used were the same as those employed for producing welds in Alclad sheets (1500-rpm tool rotational speed, 5.1-mm tool plunge, and 10-s stir time). Figure 19 shows the cross-section of a spot weld produced in bare sheets. As can be seen, no major differences were observed with regard to bond width and hook height between the welds made in bare sheets and Alclad sheets. Lap-shear tests on the welds produced in 2014-T4 bare sheets yielded a very similar average failure load to the welds produced in 2014-T4 Alclad sheets (Table 4). The failure mode was also very similar in welds produced in bare sheets and Alclad sheets. Studies thus show that FSSW works well for joining aluminum sheets, bare, or Alclad. This is a particularly useful capability of the process as many aluminum alloys are industrially used in Alclad condition, especially in the aerospace industry. There is, however, one potential concern in using FSSW for joining Alclad sheets. As can be seen in Fig. 13, friction between the tool shoulder and the upper sheet top surface results in removal of the Alclad layer (over the entire area under the tool shoulder). Similarly, the exit whole surfaces are also not covered with the Alclad layer. These regions of the weld are thus susceptible to corrosion. Further, galvanic coupling between the unprotected weld region and the surrounding Alclad base material can result in severe weld corrosion.

In another round of experiments, spot welds were produced in 3-mm thick 2014 Alclad sheets in T6 condition. The tool and process parameters used were the same as those employed for making welds in 2014-T4 sheets. Microstructural examination of the welds produced in the T6 base material indicated that they were as good as those made in the T4 base material (Fig. 20). Lap-shear tests on these welds also indicated the same (Table 4). Microhardness measurements (Table 5), however, revealed some differences between the welds made in T4 and T6 conditions, especially in the HAZ. As can be seen, the
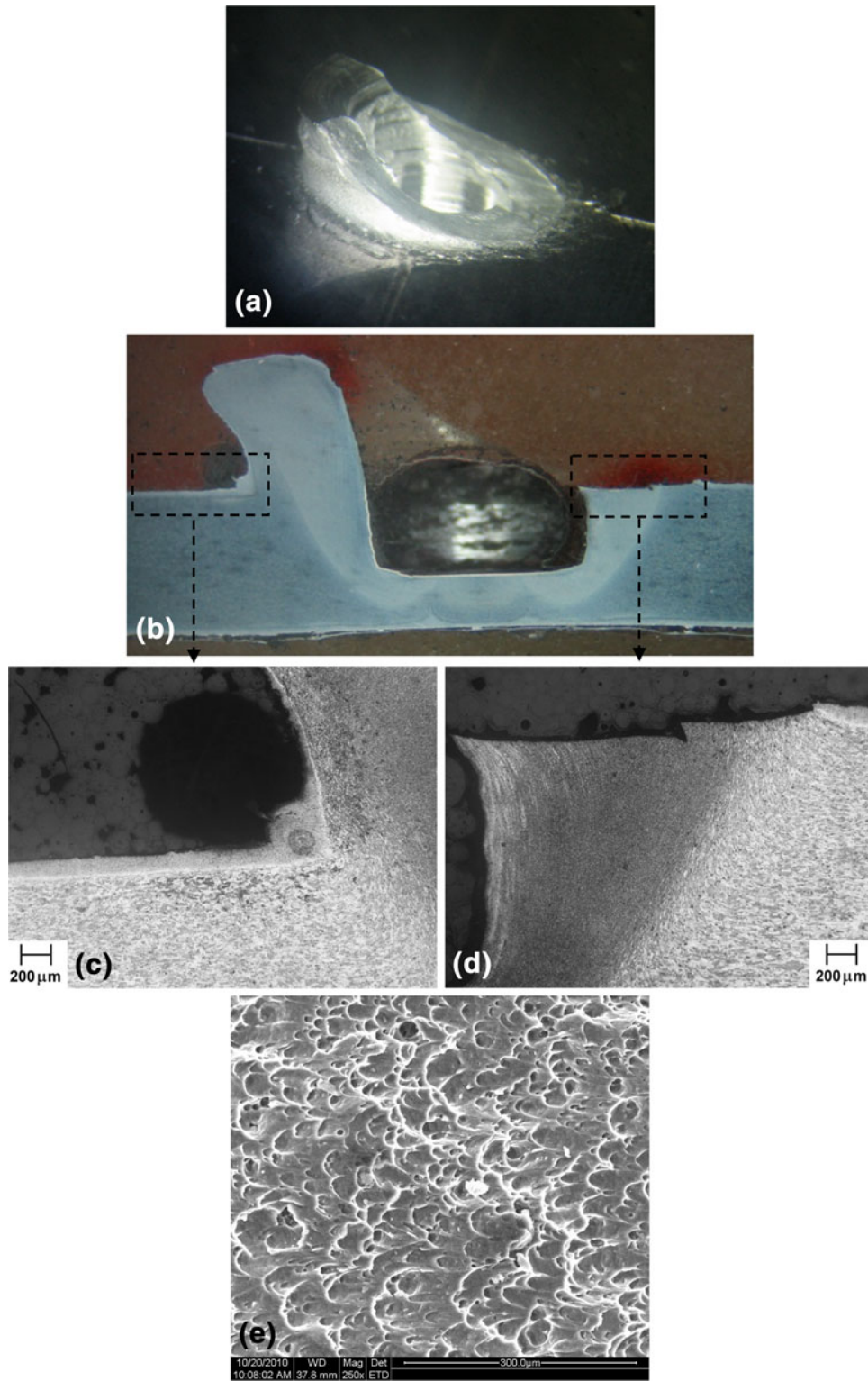
Fig. 17 Failure mode in friction stir spot welds under lap-shear loading: (a) photograph of the failed weld as seen on the lower sheet, (b) polished and etched cross-section of the failed weld shown in (a), (c) and (d) higher magnification optical micrographs corresponding to the boxed regions marked in (b), (e) SEM secondary electron image showing the fracture features in the final fracture portion

SZ hardness is more or less the same in the welds produced in T4 and T6 conditions. In both cases, the SZ hardness is lower than the hardness of the respective base materials. While the difference between the SZ and the base material hardness is not much in the case of T4, the difference is significant in the case of T6.
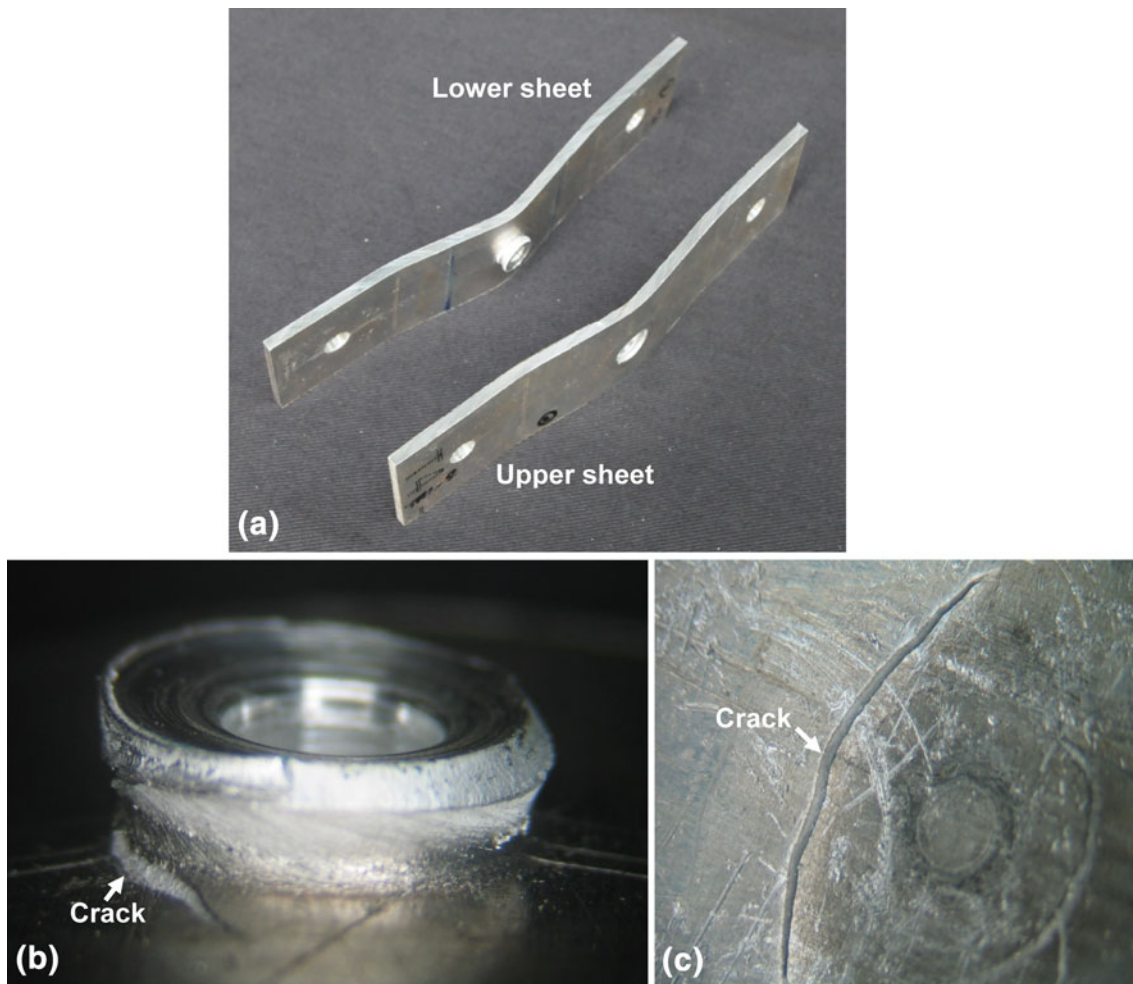
Fig. 18 Failure mode in friction stir spot welds under cross-tension loading: (a) photograph of the failed specimen, (b) crack around the weld circumference as seen on the lower sheet top surface, and (c) crack as seen on the lower sheet bottom surface
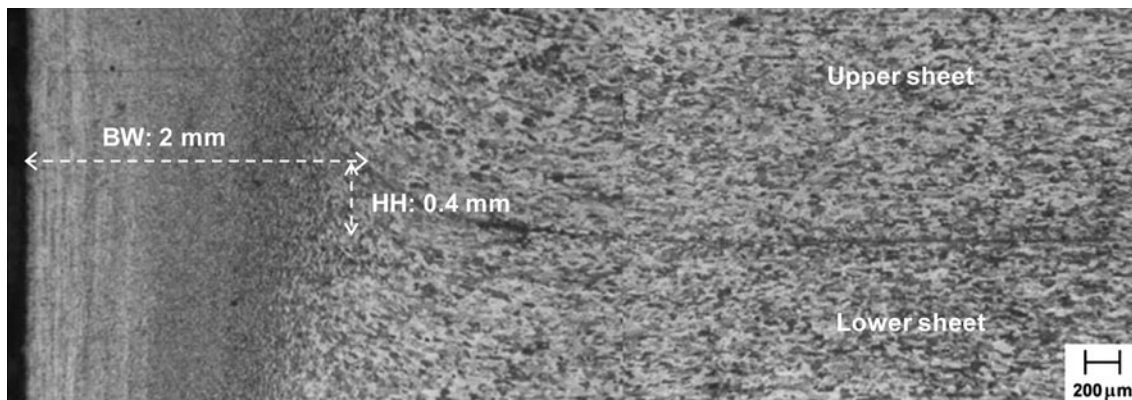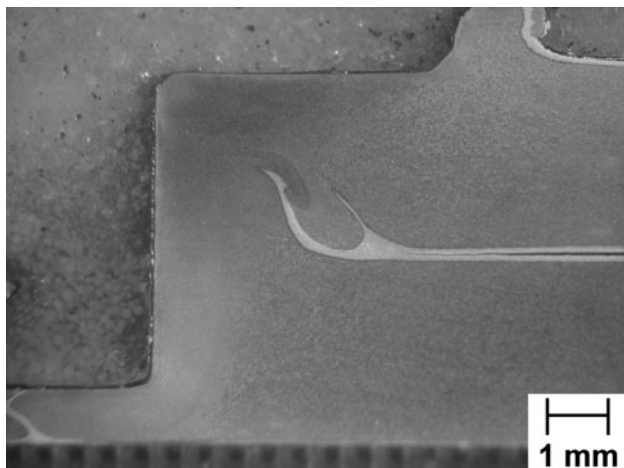

Fig. 19 Microstructure of a friction stir spot weld in alloy 2014-T4 without Alclad

During FSSW, the temperatures attained in the SZ are well above the solvus temperatures of GP zones (in the case of T4 base material) or λ' and θ' strengthening precipitates (in the case of T6 base material). Further, in the case of alloy 2014, irrespective of the base material temper condition, the thermal cycle involved in FSSW can result in formation of some equilibrium λ and θ phases in the SZ (Ref 28-30). Another effect to be considered is fragmentation of the second-phase particles originally present in the base material. These second-phase particles as well as the equilibrium phases that form in

the SZ in-situ can undergo partial dissolution during the process. During cooling from high temperatures, additional formation and/or coarsening of the equilibrium phases is also possible. In short, t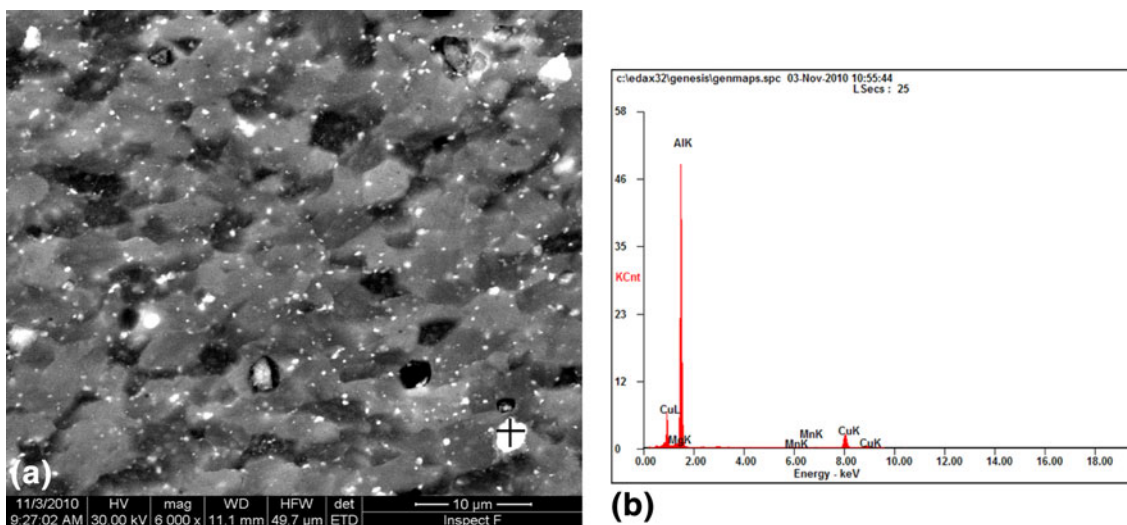he overall response in the SZ includes a combination of dissolution, coarsening, and reprecipitation of strengthening precipitates during welding (Ref 30). In the current study, SEM examination of the weld SZs in T4 and T6 base materials revealed very similar microstructural features (Fig. 21), with very fine, recrystallized equiaxed grains (average grain size ~2 μm), and a large number of uniformly distributed Cu-rich equilibrium second phases (most of these particles were <1 μm in size, but there were a few coarser (2-4 μm) particles). These observations are consistent with the findings of earlier investigations on friction stir welding of Al-Cu alloys (Ref 28, 30, 37). Clearly, whether the base material is in T4 or T6 condition, the SZ can be expected to be devoid of proper strengthening precipitation in as-welded condition. The SZ, however, can respond, although not as strongly as the standard solution treated material, to natural or artificial aging treatments. The welds made in the current study in T4 and T6 base materials would have undergone natural aging before the hardness measurements were made. Based on the above, it can be understood why the SZ hardness is more or less the same in welds made in T4 and T6 conditions and why the SZ hardness is lower compared to the base materials. Similarly, the thermal cycles involved in FSSW can result in overaging of strengthening precipitates in the HAZ (Ref 28, 30). It is well-known that HAZ overaging is a lesser problem in welding of heat-treatable aluminum alloys in T4 condition than in T6 condition (Ref 27). This explains why, in the current study, the HAZ of the T6 base material showed somewhat lower hardness compared to that in the T4 base material.

It is interesting to note that despite considerable differences in the HAZ microstructure between the welds made in T4 and T6 conditions, the welds showed a very similar lap-shear performance. This indicates that the mechanical properties of a friction stir spot weld are governed more by the geometrical aspects (hook height and bond width) of the weld and are less sensitive to the extent of microstructural damage in the HAZ, which is dependent on the base material temper condition. Overall, the current study shows that FSSW can produce equally strong joints in alloy 2014 in T4 and T6 conditions.

Fig. 20 Macrostructure of a friction stir spot weld in alloy 2014-T6 Alclad sheets

Table 5 Results of Vickers microhardness tests (average of 10 measurements in each case)

Condition	Base material	Spot weld	
		SZ	HAZ
T4	104 ± 5	98 ± 5	82 ± 3
T6	116 ± 6	100 ± 7	76 ± 4

Fig. 21 (a) SEM secondary electron image of the SZ in alloy 2014-T4 and (b) EDS spectrum of a second-phase particle in the SZ

4. Conclusions

1. Achieving satisfactory friction stir spot welds requires careful choice of tool geometry and process parameters for a given material and sheet thickness combination. In the current study, optimum tool geometry, and process parameters were established for 3-mm thick sheet of aluminum alloy 2014. A good basis for process optimization is "maximize bond width and minimize hook height."
2. Friction stir spot welds outperform riveted joints by a considerable margin under lap-shear and cross-tension loading. FSSW can thus provide a superior alternative to riveting for fabrication of aluminum sheet metal structures.
3. The mechanical performance of a friction stir spot weld is mainly governed by its geometrical features (hook height and bond width).
4. Alclad aluminum sheets are as conducive to FSSW as bare aluminum sheets. Alclad sheets present no special problems in FSSW.
5. Mechanical properties of friction stir spot welds are not very sensitive to the base material temper condition; equally strong joints can be produced in alloy 2014 in T4 and T6 conditions.

Acknowledgments

References

1. T. Iwashita, Method and Apparatus for Joining. US Patent 6601751 B2, Aug. 2003
2. R. Sakano, K. Murakami, K. Yamashita, T. Hyoe, M. Fujimoto, M. Inuzuka, Y. Nagao, and H. Kashiki, Development of Spot FSW Robot System for Automobile Body Members, 3rd International Symposium of Friction Stir Welding, Kobe, Japan, TWI, Sept. 27-28, 2001
3. C. Shilling and J. dos Santos, Method and Device for Joining at Least Two Adjoining Work Pieces by Friction Welding, US Patent Application 2002/0179682
4. K. Okamoto, F. Hunt, and S. Hirano, Development of Friction Stir Welding Technique and Machine for Aluminum Sheet Metal Assembly—Friction Stir Welding of Aluminum for Automotive Applications, SAE World Congress, 2005-01-1254, April 11-14, 2005
5. H. Badarinarayan, F. Hunt, and K. Okamoto, Friction Stir Spot welding, *Friction Stir Welding and Processing*, R.S. Mishra and M.W. Mahoney, Ed., ASM International, Materials Park, 2007, p 235–272
6. H.J. Liu, H. Fujii, M. Maeda, and K. Nogi, Tensile Properties and Fracture Locations of Friction-Stir-Welded Joints of 2017-T351 Aluminum Alloy, *J. Mater. Process. Technol.*, 2003, **142**, p 692–696
7. A. Gerlich, P. Su, M. Yamamoto, and T.H. North, Effect of Welding Parameters on the Strain Rate and Microstructure of Friction Stir Spot Welded 2024 Al Alloy, *J. Mater. Sci.*, 2007, **42**, p 5589–5601
8. H. Badarinarayan, Y. Shi, X. Li, and K. Okamoto, Effect of Tool Geometry on Hook Formation and Static Strength of Friction Stir Spot Welded Aluminum 5754-O Sheets, *Int. J. Mach. Tools Manuf.*, 2009, **49**, p 814–823
9. T.A. Freeney, S.R. Sharma, and R.S. Mishra, Effects of Welding Parameters on Properties of 5052 Al Friction Stir Spot Welds, SAE Special Publication, SP-2034, SAE 2006-01-0969, Warrendale, USA, 2006
10. S. Lathabai, M.J. Painter, G.M.D. Cantin, and V.K. Tyagi, Friction Spot Joining of an Extruded Al-Mg-Si Alloy, *Scr. Mater.*, 2006, **55**, p 899–902
11. Y. Uematsu, K. Tokaji, Y. Tozaki, T. Kurita, and S. Murata, Effect of Re-Filling Probe Hole on Tensile Failure and Fatigue Behaviour of Friction Stir Spot Welded Joints in Al-Mg-Si Alloy, *Int. J. Fatigue*, 2008, **30**(10–11), p 1956–1966
12. P.C. Lin, J. Pan, and T. Pan, Failure Modes and Fatigue Life Estimations of Spot Friction Welds in Lap-Shear Specimens of Aluminum 6111-T4 Sheets—Part 1: Welds Made by a Concave Tool, *Int. J. Fatigue*, 2008, **30**(1), p 74–89
13. A. Gerlich, G.A. Cingara, and T.H. North, Stir Zone Microstructure and Strain Rate During Al 7075-T6 Friction Stir Spot Welding, *Metall. Mater. Trans. A*, 2006, **37A**, p 2773–2786
14. Y. Tozaki, Y. Uematsu, and K. Tokaji, Effect of Processing Parameters on Static Strength of Dissimilar Friction Stir Spot Welds Between Different Aluminium Alloys, *Fatigue Fract. Eng. Mater. Struct.*, 2007, **30**(2), p 143–148
15. V.X. Tran, J. Pan, and T. Pan, Effects of Processing Time on Strengths and Failure Modes of Dissimilar Spot Friction Welds Between Aluminum 5754-O and 7075-T6 Sheets, *J. Mater. Process. Technol.*, 2009, **209**(8), p 3724–3739
16. P. Su, A. Gerlich, T.H. North, and G.J. Bendzsak, Energy Utilisation and Generation During Friction Stir Spot Welding, *Sci. Technol. Weld. Joining*, 2006, **11**(2), p 163–169
17. A. Gerlich, P. Su, and T.H. North, Peak Temperatures and Microstructures in Aluminum and Magnesium Alloy Friction Stir Spot Welds, *Sci. Technol. Weld. Joining*, 2005, **10**(6), p 647–652
18. P. Su, A. Gerlich, T.H. North, and G.J. Bendzsak, Material Flow During Friction Stir Spot Welding, *Sci. Technol. Weld. Joining*, 2005, **11**(1), p 61–71
19. M. Awang, V.H. Mucino, Z. Feng, and S.A. David, Thermo-Mechanical Modeling of Friction Stir Spot Welding (FSSW) Process: Use of an Explicit Adaptive Meshing Scheme, SAE World Congress, 2005-01-1251, April 11-14, 2005
20. Y.H. Yin, N. Sun, T.H. North, and S.S. Hu, Hook Formation and Mechanical Properties in AZ31 Friction Stir Spot Welds, *J. Mater. Process. Technol.*, 2010, **210**(14), p 2062–2070
21. Y.H. Yin, A. Ikuta, and Y.H. North, Microstructural Features and Mechanical Properties of AM60 and AZ31 Friction Stir Spot Welds, *Mater. Des.*, 2010, **31**(10), p 4764–4776
22. Z. Feng, M.L. Santella, S.A. David, R.J. Steel, S.M. Packer, T. Pan, M. Kuo, and R.S. Bhatnagar, Friction Stir Spot Welding of Advanced High-Strength Steels—A Feasibility Study, SAE World Congress, 2005-01-1248, April 11-14, 2005
23. V.X. Tran and J. Pan, Fatigue Behavior of Dissimilar Spot Friction Welds in Lap-Shear and Cross-Tension Specimens of Aluminum and Steel Sheets, *Int. J. Fatigue*, 2010, **32**(7), p 1167–1179
24. L. Agarwal, P.K. Mallick, and H.T. Kang, Spot Friction Welding of Mg-Mg, Al-Al and Mg-Al Alloys, SAE Technical Paper No. 2008-01-0144, Warrendale, PA, USA, 2008
25. Y. Tozaki, Y. Uematsu, and K. Tokaji, Effect of Tool Geometry on Microstructure and Static Strength in Friction Stir Spot Welded Aluminium Alloys, *Int. J. Mach. Tools Manuf.*, 2007, **47**(15), p 2230–2236
26. A.C. Addison and A.J. Robelou, Friction Stir Spot Welding: Principal Parameters and their Effects, 5th International Symposium on Friction Stir Welding, 2004, Metz, France
27. S. Kou, *Welding Metallurgy*, 2nd ed., Wiley, Hoboken, NJ, 2003
28. R. Nandan, T. DebRoy, and H.K.D.H. Bhadeshia, Recent Advances in Friction-Stir Welding – Process, Weldment Structure and Properties, *Prog. Mater. Sci.*, 2008, **53**, p 980–1023
29. I. Dutta, C.P. Harper, and G. Dutta, Role of Al_2O_3 Particulate Reinforcements on Precipitation in 2014 Al-Matrix Composites, *Metall. Mater. Trans. A*, 1994, **25A**, p 1591–1602
30. R.S. Mishra and Z.Y. Ma, Friction Stir Welding and Processing, *Mater. Sci. Eng. R*, 2005, **50**, p 1–78
31. H. Badarinarayan, Q. Yang, and S. Zhu, Effect of Tool Geometry on Static Strength of Friction Stir Spot-Welded Aluminum Alloy, *Int. J. Mach. Tools Manuf.*, 2009, **49**, p 142–148
32. S. Hirasawa, H. Badarinarayan, K. Okamoto, T. Tomimura, and T. Kawanami, Analysis of Effect of Tool Geometry on Plastic Flow During Friction Stir Spot Welding Using Particle Method, *J. Mater. Process. Technol.*, 2010, **210**, p 1455–1463
33. Q. Yang, S. Mironov, Y.S. Sato, and K. Okamoto, Material Flow During Friction Stir Spot Welding, *Mater. Sci. Eng. A*, 2010, **527**, p 4389–4398

34. G. Buffa, J. Hua, R. Shivpuri, and L. Fratini, Design of the Friction Stir Welding Tool Using the Continuum Based FEM Model, *Mater. Sci. Eng. A*, 2006, **419**(1–2), p 381–388

35. D. Mitlin, V. Radmilovic, T. Pan, J. Chen, Z. Feng, and M.L. Santella, Structure-Properties Relations in Spot Friction Welded (also Known as Friction Stir Spot Welded) 6111 Aluminum, *Mater. Sci. Eng. A*, 2006, **441**(1–2), p 79–96

36. P.C. Lin, J. Pan, and T. Pan, Failure Modes and Fatigue Life Estimations of Spot Friction Welds in Lap-Shear Specimens of Aluminum 6111-T4 Sheets—Part 2: Welds Made by a Flat Tool, *Int. J. Fatigue*, 2008, **30**, p 90–105

37. Y.C. Chen, J.C. Feng, and H.J. Liu, Precipitate Evolution in Friction Stir Welding of 2219-T6 Aluminum Alloys, *Mater. Charact.*, 2009, **60**(6), p 476–481